

Deconvolution of Squared Velocity Waveform as Applied to the Study of a Noncoherent Short-period Radiator in the Earthquake Source

A. A. GUSEV¹ and V. M. PAVLOV¹

Abstract—We consider an inverse problem of determination of short-period (high-frequency) radiator in an extended earthquake source. This radiator is assumed to be noncoherent (i.e., random), it can be described by its power flux or brightness (which depends on time and location over the extended source). To decide about this radiator we try to use temporal intensity function (TIF) of a seismic waveform at a given receiver point. It is defined as (time-varying) mean elastic wave energy flux through unit area. We suggest estimating it empirically from the velocity seismogram by its squaring and smoothing. We refer to this function as “observed TIF”. We believe that one can represent TIF produced by an extended radiator and recorded at some receiver point in the earth as convolution of the two components: (1) “ideal” intensity function (ITIF) which would be recorded in the ideal nonscattering earth from the same radiator; and (2) intensity function which would be recorded in the real earth from unit point instant radiator (“intensity Green’s function”, IGF). This representation enables us to attempt to estimate an ITIF of a large earthquake by inverse filtering or deconvolution of the observed TIF of this event, using the observed TIF of a small event (actually, fore- or aftershock) as the empirical IGF. Therefore, the effect of scattering is “stripped off”. Examples of the application of this procedure to real data are given. We also show that if one can determine far-field ITIF for enough rays, one can extract from them the information on space-time structure of the radiator (that is, of brightness function). We apply this theoretical approach to short-period *P*-wave records of the 1978 Miyagi-oki earthquake ($M = 7.6$). Spatial and temporal centroids of a short-period radiator are estimated.

Key words: Noncoherent radiator, radiation intensity, intensity deconvolution procedure.

1. Introduction

For many years, in accordance with physical intuition, seismologists believe that radiators of long-period and short-period waves in an earthquake source practically coincide. This is actually a hypothesis which merits testing, but such a test requires a technique to study short-period (SP) radiator separately. This problem cannot be solved in frames of a traditional approach to source inversion which is based on a linear relation between source-slip rate and far-field displacement (see KOSTROV and DAS, 1988) because fine details of space-time source structure cannot be

resolved in principle. Here, an alternative approach is suggested, which is based on the assumption of a linear relation between source power flux (or brightness) and far-field wave intensity. Instead of the usual additivity of amplitudes we employ additivity of power. This additivity is a hypothesis concerning properties of a real source which cannot be formally proved, meaning that we assume a noncoherent nature of SP radiator. In other words, we assume that the source can be thought of as consisting of many independently radiating spots so that contributions of any pair of spots into far-field amplitude are uncorrelated. The process of scattering of source radiation in the earth produces coherent (as in the case of such deterministic phases as pP and sP) as well as noncoherent (coda) components of seismogram of a point source, but assumed initial randomness of radiation of a large source will be preserved in seismic records. This fact justifies the application of linear inversion methods to intensity; therefore, we use them (in particular inverse filtering and linear least squares) below. In general, SP body wave seismogram reflects the source space-time function as well as the actual medium response produced by scattering (here we use the term “scattering” loosely to cover both scattered and converted waves). Both (source and medium) components will be treated as random signals and be specified by their mean square amplitudes. Therefore, the main variable below will be squared particle velocity u^2 ; multiplied by $c\rho$ (c : wave speed, ρ : density) it gives true intensity (W/m^2). Intensity as a function of time will be named temporal intensity function (TIF).

We begin with the “ideal” TIF (or ITIF) defined as the one that will be recorded at a far-field receiver situated on a given ray at unit distance from an extended source in the “ideal earth” with no scattering. Consider also “intensity Green’s function” (IGF) or TIF produced by unit source and recorded on the same ray at a given distance in the real scattering medium. Now the TIF function recorded in real earth can be represented simply as convolution of ITIF and IGF. Now if IGF and TIF are known, one can try to determine ITIF by inverse filtering or deconvolution.

KOPNICHEV (1977) was the first to suggest an approach of this kind for a special hypothetical case when IGF can be described analytically as exponent plus delta function. Below we shall instead employ the empirical estimate of IGF based on a record of a small-magnitude event.

After filtering off the effect of scattering from several records of the same earthquake one can try to study the space-time structure of the radiator of SP energy (PAVLOV and GUSEV, 1980). IIDA and HAKUNO (1984) were the first to design a technique of such kind. They successfully used accelerograms of large earthquakes (TOKACHI-OKI, 1968 and MIYAGI-OKI, 1978) and also of small shocks to reconstruct a “source brightness” field over a 3D ($X \times Y \times T$) sub-source grid. In the present paper we shall use teleseismic P -wave records as initial data and shall specify a source by its power moments.

2. Direct and Inverse Problem for Radiation Intensity; General Theory and Application for Teleseismic P Waves

Let us consider the relation between brightness of a noncoherent body wave radiator and radiation intensity at a recording point. Below we shall implicitly consider the radiation field of some definite frequency band Δf around central frequency f_0 . If radiation pattern is the same for any element dS of flat surface Σ of radiator, one can introduce scalar brightness function $P(\vec{x}, t)$ so that $P(\vec{x}, t) dS$ is power flux from dS (dS is located at \vec{x} ; $\vec{x} = 0$ is the hypocenter) at a time t . Now introduce IGF and let $W_1(\vec{y}, t - \tau)$ be radiation intensity at \vec{y} at a time $(t - \tau)$ produced by unit energy burst at $\vec{x} = 0$ at a moment τ (W_1 includes radiation pattern factor).

Assume also that if the unit source is shifted to a point $\vec{x} \neq 0$, its intensity pulse shape does not change so that it can be expressed as $W_1(\vec{y}, t - \tau + \vec{x} \cdot \vec{r}/c)$ where $\vec{r} = \vec{y}/|\vec{y}|$. Then intensity $dW(\vec{y}, t)$ produced at \vec{y} by a source element located on dS at \vec{x} can be expressed as

$$dW(\vec{y}, t) = \int_{-\infty}^{\infty} W_1(\vec{y}, t - \tau + \vec{x} \cdot \vec{r}/c) P(\vec{x}, \tau) d\tau dS. \quad (1)$$

Total intensity at \vec{y} can be found by integration over Σ :

$$W(\vec{y}, t) = \int_{-\infty}^{\infty} W_1(\vec{y}, t - \tau') I(\vec{r}, \tau') d\tau', \quad (2)$$

where

$$I(\vec{r}, \tau') = \int_{\Sigma} P(\vec{x}, \tau' + \vec{x} \cdot \vec{r}/c) dS \quad (3)$$

is the aforementioned ITIF (cf., RICE, 1980, Eq. (4.3)).

The presented simple derivation allowed us to obtain useful formulas but it is not at all rigorous. Strictly speaking, dS and $d\tau$ in (1) cannot be arbitrary small but must be close to $\Delta S \approx R_c^2$ (GUSEV, 1983) and $\Delta\tau = 2T_c$ respectively, where R_c and T_c are so-called correlation radius and correlation time of a source (for given f_0). That is, values of source-slip rate function at space-time points (\vec{x}, t) and (\vec{x}', t') are uncorrelated if $|\vec{x} - \vec{x}'| \gg R_c$ or $|t - t'| \gg T_c$. Though integral representation (2) fails in a strict sense, it stays, however, valid approximately in case $R_c \ll L$ and $T_c \ll T$, where L and T are source length and duration. Note that $T_c > 1/\Delta f$ and $R_c > c/\Delta f$ (c is the wave speed) so that Δf cannot be arbitrarily small. Another complication is related to definition of intensity. Theory deals with ensemble mean of variance of amplitude while in application one must use instead the smoothed observed squared amplitude (short-term temporal average) which can be rather noisy estimate of the first.

Inversion procedure for brightness function $P(\vec{x}, t)$ consists of two steps: (1) determination of ITIF for several rays and (2) reconstruction of $P(\vec{x}, t)$ from these

functions. At the first step we shall proceed from relation (2) which can be considered as an integral equation with respect to $I(\vec{r}, t)$. It can be solved by inverse filtering if $W(y, t)$ and $W_1(y, t)$ are known. In practice we can estimate W from a seismogram but W_1 is unknown. We can infer, however, that the recorded intensity of a small shock (with low magnitude L and T) can be considered as an empirical version of W_1 . To be applicable for this aim, a small event must have its hypocenter and fault plane mechanism close to those of a large event. In the case of teleseismic P -wave data, epicenters are not very important and proximity of depths is critical. Because of finite L and T of a small shock, simple deconvolution cannot provide a stable estimate of W . However, some smoothed version of W can be sought for. Thus, in practical algorithm we shall combine inverse filtering in frequency domain (dividing spectra of TIF of a large event by that of a small event) and smoothing, or high-cut filtering. We shall name this procedure “intensity deconvolution”. The use of smoothing operator mentioned above can somewhat weaken the condition on depth coincidence because very accurate phasing becomes senseless. If the time constant of smoothing is τ_s , then one can assume the values of depth difference between small shock and any point of extended source of large shock permissible up to $c^*\tau_s$, where c^* is an appropriate speed factor. For the important case of pP wave, $c^* = c_p/2 \approx 3$ km/s, for sP , $c^* = (c_p + c_s)/4 \approx 2.5$ km/s. Thus, if, for example, τ_s is 5–10 s, depth differences reaching 20–25 km can be permissible. To minimize errors, small event depth should near the middle of the possible depth range of a large event (which can deduced, e.g., from aftershock data).

The second step of inversion departs from relation (3) written for several rays. One, for instance, can use some functional form for $P(\vec{x}, t)$ *a priori* and seek its parameters. We prefer power moment approach to source description (GUSEV and PAVLOV, 1988) which uses no *a priori* assumptions on functional form of $P(\vec{x}, t)$. In this paper we shall limit ourselves by first degree moments.

Let e_k be the normalized first temporal moment of ITIF of P waves, that is retardation of intensity pulse centroid with respect to P wave arrival, at k -th seismic station. Let $(M_1 M_2 M_3)$ be the vector from the hypocenter to the brightness centroid, and M_t be the average (over the source) retardation of radiation with respect to origin time. Assume axes (1, 2, 3) to be chosen as (north, east, up). Now, for k -th station (Eq. (3)) leads to relation (GUSEV and PAVLOV, 1988):

$$M_t - (r_{1k}M_1 + r_{2k}M_2 + r_{3k}M_3)/c_p = e_k, \quad (4)$$

where \vec{r}_k is the unit ray vector from the hypocenter to the k -th station. Formally, when e_k are known for 4 or more stations, the system of equations (4) can be solved by least squares to provide estimates of M_1 , M_2 , M_3 , and M_t . However, in the case of teleseismic P waves the situation is not so simple. Note that \vec{r}_k is close to vertical for any teleseismic record; this means that estimates of M_t and M_3 become almost linearly dependent, so one practically cannot determine both M_t and M_3 .

Additional constraint must be added. The simplest one is $M_3 = 0$ which was, in fact, used in this paper. Its use can be correct only when one believes that M_3 is much lower than $(M_1^2 + M_2^2)^{0.5}$. In practice this can be expected when the horizontal extent of a source is much larger than the vertical one. This is often the case with large shallow earthquakes, and at least in these cases the application of the suggested approach seems to be justified.

3. Data and Processing Procedure

The theoretical approach described above was tested using records of SP instruments of the Soviet (ESSN) and WWSSN seismic nets. We studied two large earthquakes: Miyagi-oki, Japan (June 12, 1978, $M = 7.6$) and the S. Kurile event of March 24, 1978 ($M = 7.7$). We have chosen: the foreshock ($M = 5.5$) that occurred 8 min before the main Miyagi-oki event and the aftershock of the March 24 event that occurred on March 25 at 05 h 24 m ($M = 5.1$) as small events. The fault plane solution of foreshock and mainshock of the Miyagi-oki event practically coincide (SENO *et al.*, 1980). As for the depth, $h = 28$ km for mainshock hypocenter, $h = 26$ km for foreshock, and the mainshock extended source depth range, as can be judged from the aftershock pattern, is $h = 15-50$ km (or in the range of ± 22 km from hypocentral depth) (SENO *et al.*, 1980). These figures should be compared with the horizontal extent of the aftershock zone, which is about 70 km. Thus, all three conditions of applicability of the proposed technique (on radiation pattern, depth difference, and horizontal elongation) are more or less satisfied. For the Kurile events, fault planes could not be compared, and both depths are shallow. Data selection met large problems because of the narrow dynamic range of photo records. Thus we could collect the sufficient number of records only for the Miyagi-oki event. The records were digitized with the time step of 0.09 s. Examples of records are given in Figure 1.

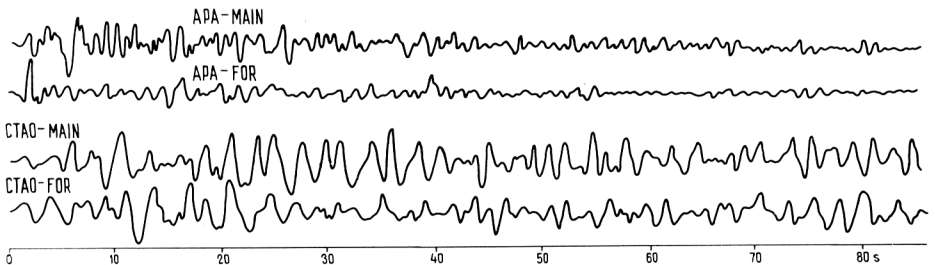


Figure 1

Records of the main shock and foreshock of Miyagi-oki earthquake in opposite azimuths, at stations APA (335°) and CTAO (178°). Channels are SKM-3 (z) at APA and SRO-SP(Z) at CTAO. All vertical scales are arbitrary here and below, time scale starts at P wave onset.

Intensity deconvolution procedure for each station consisted of the following steps:

1. TIF estimate of the main shock. This includes:
 - 1.1. Cut out a piece of P wave record of a given duration (usually of about 80 s).
 - 1.2. Apply band filtering with a given band position and band width.
 - 1.3. TIF estimate as a sum of squares of a signal and its Hilbert transform.
2. TIF estimate of the small shock (same way as in 1).
3. ITIF estimate of the main shock. This includes:
 - 3.1. Compute TIF spectra of the main shock ($S_m(f)$) and of TIF of the small shock ($S_a(f)$).
 - 3.2. Perform inverse filtering according to formula:

$$g(f) = \frac{S_m(f)S_a^*(f)}{S_a(f)S_a^*(f) + \varepsilon^2 \max_f(S_a(f)S_a^*(f))}, \quad (5)$$

where an asterisk denotes the complex conjugation and stabilizing parameter ε^2 limits g when $S_a(f)S_a^*(f)$ is near zero.

- 3.3 Perform low-pass (zero-phase) filtering over $g(f)$ with high cutoff frequency FHC.
- 3.4. Pass to the time domain getting $g(t)$ and observe the results. Change ε^2 and FHC and go to 3.2 if needed.
- 3.5. Compute normalized temporal moments of $g(t)$. Degree k moment is:

$$E_k = \int_{t_1}^{t_2} g(t)(t - t_0)^k dt, \quad (6)$$

where interval (t_1, t_2) contain source pulse, t_0 is P onset time, and degree 1 normalized moment is $e = E_1/E_0$.

Note that when P onsets of large and small shocks are at the same position in corresponding time series, $t_0 = 0$. Zero-phase high-cutoff filtering does not change e but produces nonzero energy at negative t ; this artifact adds no real problem, but t_1 becomes negative.

During data processing we used band-filtered seismogram instead of “true” band-filtered velocity. In a more accurate approach one could carry out inverse filtering to account for instrument and medium absorption and pass to “true” velocity; all these operations in fact have a minor effect on the shape of smoothed squared band-filtered amplitude.

Note also that in practice we need not apply the smoothing operator to the “observed” intensity estimates, because during division in (5) this operator cancels. Smoothing is applied, however, to demonstration examples.

The described procedure is illustrated by Figure 2 which presents a typical example. For the March 24, 1978 event at station Iultin (ILT) we show two pairs of the observed TIF for two frequency bands and estimates of ITIF. One can see

M=7.7 March 24.1978 IUL

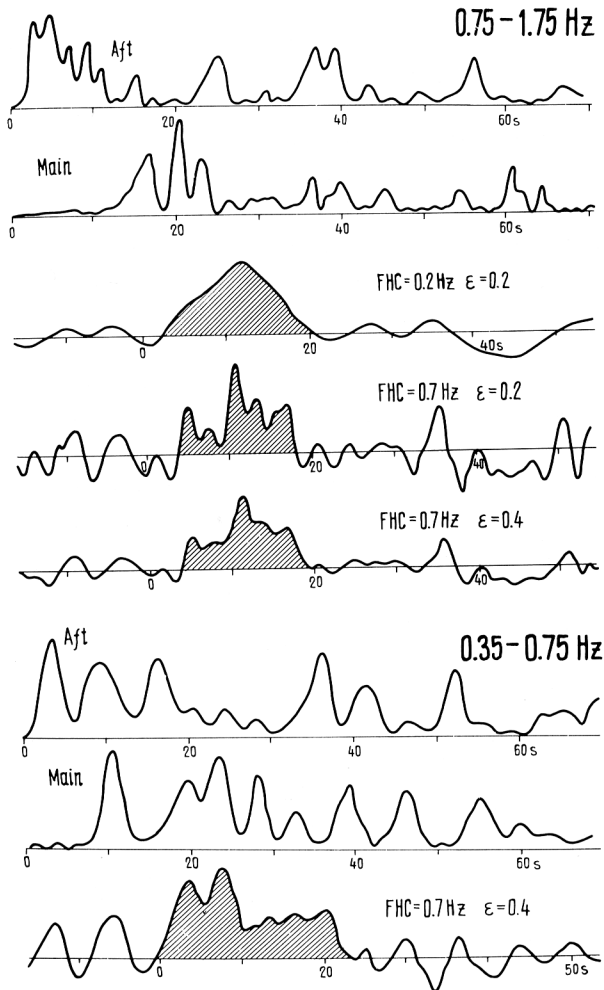


Figure 2

Processing of the records of the March 24, 1978 event and its aftershock at ILT. From top to bottom: temporal intensity from records of aftershock and main shock, for frequency band of 0.75-1.75 Hz; Three ITIF estimates obtained using various combinations of control parameters (see text); record of TIF and ITIF estimates for the band of 0.35-0.75 Hz.

that a certain selection of ϵ^2 and FHC control parameters can provide "reasonable" pulse shape of ITIF, but actually this shape cannot be determined even marginally reliable. One can note, however, that variation of control parameters cannot markedly change such characteristics of the ITIF pulse as duration and temporal centroid position, so one can try to use these in further studies.

4. Study of Miyagi-oki Event

In Figure 3 we present estimated ITIF for Miyagi-oki event, for frequency band of 0.45–1.5 Hz. Smoothing operator was used with $FHC = 0.15$ Hz, its τ_s near 7 s in accordance with preliminary estimates of correct τ_s for a depth difference extending to 22 km, and ε^2 of 0.1. Again we consider any particular details of pulse shapes as unreliable, but we believe that the values of e_k can be determined more or less accurately. These estimates are given in Table 1. Their accuracy is not very high because some subjective judgement was needed in order to cut out “true pulse” from “background noise”, and errors of this judgement could lead to errors of estimated centroid position.

The “observed” e_k values determined in this way were substituted to the system of equations (4) with condition $M_3 = 0$ and M_1, M_2 , and M_t were found by least squares. The following estimates were then obtained (at $c_p = 6$ km/s): $M_1 = 34 \pm 18$ km; $M_2 = -21 \pm 29$ km; $M_t = 14 \pm 1.5$ s, and rms residual (goodness of fit) was about 3 s. Thus, the centroid of noncoherent radiator of seismic energy of 0.45–1.5 Hz frequency band was situated at about 40 km to NNW from hypocenter. In Figure 4 this result is compared with the results of the previous studies of the same event; a reasonable agreement can be seen.

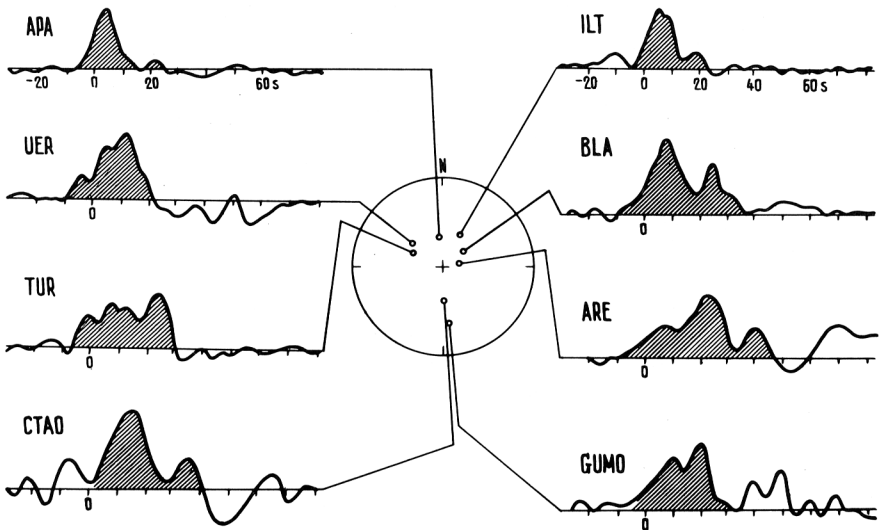


Figure 3

Estimated ITIF of P waves for Miyagi-oki event at eight stations. Frequency band is 0.45–1.5 Hz. Ray directions on the lower hemisphere are shown in the center. Integration area used while estimation of e_k is hatched.

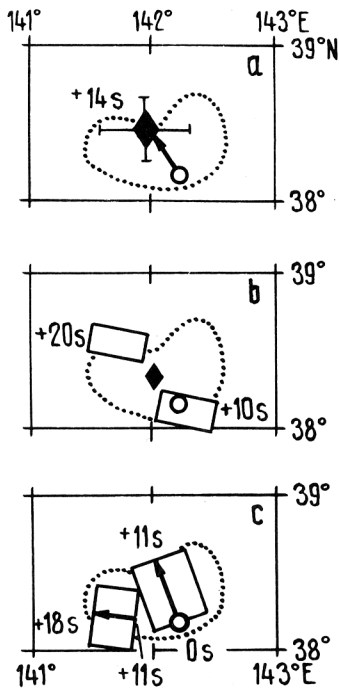


Figure 4

Space-time representation of the source of the Miyagi-oki event. The circle is the epicenter, a dot line indicates the aftershock zone. a: centroid of “0.5–1.5 Hz radiator” (this paper, diamond). Number is the value of temporal centroid. b: acceleration power radiator reconstructed by IIDA and HAKUNO (1984). Rectangles are the two brightest spots of the source, their retardation times are also given. Diamond is approximate source centroid (our estimate that is based on Figure 18 of the mentioned paper). c: long- and medium-period radiator after SENO *et al.* (1980) (“two-segment model”). For each of the two subevents of Haskell-Aki type (running stripe) start and finish times are given.

Table 1

The estimated first moment of ITIF based on records of Miyagi-oki event

Station Code	Name	Az°	Δ°	e_k, s
ILT	Iultin	23	36	8.5
BLA	Blackberg	33	95	13
ARE	Arequipa	63	70	20
GUMO	Guam	174	25	15
CTAO	Ch. Towers	176	58	17
TUR	Turgen	298	48	12
UER	Ust Elegest	308	41	10
APA	Apatity	336	61	7

5. Conclusions

We have presented the results of the first attempt to employ an intensity deconvolution approach to real data. Many points of the technique deserve deeper study, and use of photorecords prevented us from conducting a more detailed analysis of some facts. Nevertheless, we believe that our results are hopeful and that study of presumedly noncoherent short-period radiator will improve our understanding of earthquake source structure and will also provide additional information on source duration which is important for strong motion assessment.

Acknowledgement

The authors are grateful to many colleagues who assisted in the collection of seismograms.

REFERENCES

- GUSEV, A. A., and PAVLOV, V. M. (1988), *Determination of Space-time Structure of a Deep Earthquake Source by Means of Power Moments*, Tectonophysics 152, 319–334.
- IIDA, M., and HAKUNO, M. (1984), *The Difference in the Complexities between the 1978 Miyagiken-oki Earthquake and the 1968 Tokachi-oki Earthquake from a Viewpoint of the Short-period Range*, Natural Disaster Sci. 6, 1–26.
- KOPNICHEV, Yu. F. (1977), *A Method for Determination of Structure of Radiation of a Strong Earthquake by Envelope Shape of P-Wave*, Dokl. Acad. Nauk SSSR 234, 794–797 (in Russian).
- PAVLOV, V. M., and GUSEV, A. A. (1980), *On the Possibility of Reconstruction of Movement in a Deep Earthquake Source from Far-field Body Waves*, Dokl. Acad. Nauk SSSR 255, 824–829 (in Russian).
- SENO, T., SHIMAZAKI, K., SOMMERVILLE, P., and SUDO, K. (1980), *Rupture Process of the Miyagi-oki, Japan, Earthquake of June 12, 1978*, Phys. Earth Planet Interiors 23, 39–61.

(Received March 12, 1991, revised/accepted June 13, 1991)